ARTICLE

Comparison of Underwater Video with Electrofishing and Dive Counts for Stream Fish Abundance Estimation

Nathaniel P. Hitt,* Karli M. Rogers, and Craig D. Snyder
U.S. Geological Survey, Leetown Science Center, 11649 Leetown Road, Kearneysville, West Virginia 25430, USA

C. Andrew Dolloff
U.S. Forest Service and Department of Fish and Wildlife Conservation, Virginia Polytechnic Institute and State University, 1710 Research Center Drive, Blacksburg, Virginia 24060, USA

Abstract
Advances in video technology enable new strategies for stream fish research. We compared juvenile (age-0) and adult (age-1 and older) Brook Trout *Salvelinus fontinalis* abundance estimates from underwater video with those from backpack electrofishing and dive count methods across a series of stream pools in Shenandoah National Park, Virginia ($n = 41$). Video methods estimated greater mean abundance of adult trout than did one-pass electrofishing, but video estimates of adult abundance were not different than estimates from three-pass electrofishing or dive count methods. In contrast, videos underestimated the abundance of juvenile trout; we suggest that this is because predator avoidance behaviors by juvenile trout limit their use of microhabitat locations visible to cameras. Integrated abundance estimates from two cameras increased correspondence to comparison methods relative to estimates from single cameras, demonstrating the importance of an expanded field of view for video sampling in streams. Geomorphic features helped to explain methodwise differences: more adult Brook Trout were estimated with video than with three-pass electrofishing as riffle crest depth and boulder composition increased, indicating habitat associations with trout escapement from electrofishing. Our results demonstrated that video techniques can provide a robust alternative or supplement to traditional methods for estimating adult trout abundance in stream pools.

Stream fish research and management often require abundance estimation, and advances in video technology provide new strategies to achieve this goal (Struthers et al. 2015). Prior research has utilized video techniques in marine and estuarine environments to study fish species richness and abundance (Moser et al. 1998; Willis and Babcock 2000; Ebner and Morgan 2013; Holmes et al. 2013; Mallet and Pelletier 2014; Schobernd et al. 2014) and fish behavior (Brawn 1960; Myrberg et al. 1969; Trudel and Boisclair 1996; Becker et al. 2010; Coghlan et al. 2017). Video techniques also have been used in laboratory-based studies of fish behavior, habitat use, and competitive interactions (Valentin et al. 1994; Rowland et al.

1995; Castro-Santos 2005; Hitt et al. 2017; White et al. 2019) as well as to monitor movement through fish passage structures (Hatch et al. 1998; Morán-López and Tolosa 2017; Hawkins et al. 2018). By comparison, video techniques for stream fish research in situ are in their nascent stage.

Electrofishing and dive count methods are commonly used to estimate stream fish abundance (Dunham et al. 2009; Reynolds and Kolz 2012; Thurow et al. 2012), but video methods offer several potential advantages. First, electrofishing can cause fish injury or death (Snyder 2003) and can alter fish reproductive behaviors (Stewart and Lutnesky 2014), whereas video sampling has a negligible

impact and has been used to study imperiled species (Ellender et al. 2012; Feyrer et al. 2013; Chaudoin et al. 2015). Second, electrofishing materials and labor are more costly than video sampling methods (Frezza et al. 2003; Struthers et al. 2015). Third, variation in electrofishing gear performance and waveform settings (Dean et al. 2019) and netting protocols (Peterson et al. 2005) introduces uncertainty in comparisons across studies, whereas video samples provide empirical records for independent analysis. Fourth, electrofishing and dive count methods present some risk of investigator injury that is not a concern in video sampling. Moreover, video techniques can be deployed in locations where electrofishing or dive counts are not practical (Mueller et al. 2006; Weyl et al. 2013; Ebner et al. 2015; King et al. 2018).

Prior studies have shown that stream fish abundance can be estimated from video data (Frezza et al. 2003; Ellender et al. 2012; Weyl et al. 2013; Ebner et al. 2015) but that video performance will depend in part on fish body size, behavior, and environmental conditions. Frezza et al. (2003) estimated more salmonid fishes by using video than backpack electrofishing, but they found that videos were biased against detection of smaller fish. Likewise, Ellender et al. (2012) found that video-derived abundances in stream pools were more closely related to electrofishing results for a larger fish species (Eastern Cape Redfin *Pseudobarbus afer*) than for a smaller one (Cape Kurper *Sandelia capensis*). Other studies have reported that video sampling in streams underestimates abundance of nocturnal stream fishes relative to electrofishing and dive count methods (Weyl et al. 2013; Ebner et al. 2015). Limitations of video sampling in turbulent flows and structurally complex habitats have also been recognized (Frezza et al. 2003; Struthers et al. 2015; Morán-López and Tolosa 2017).

We hypothesize that limitations reported in prior research may be addressed in part by expanding the field of view in video samples. For instance, Ellender et al. (2012) used a single camera at the downstream edge of stream pools, and this may have obscured the view of fish within the upstream portions of the pool (see Frezza et al. 2003). Alternatively, cameras that are limited to the upstream portions of pools may observe energetically profitable locations for fish (Fausch 1984) but may not capture fish that are displaced further downstream in the pools (Cullen and Grossman 2019), thus leading to underestimates of total abundance. Likewise, stream habitats with complex fish cover (e.g., boulders and large woody debris) may require larger fields of view—just as additional snorkeling observers are recommended when sampling more complex stream habitats (Thurow et al. 2012). In this study, we compared fish abundance estimates between sampling methods and compared video data from single cameras against data integrated from two cameras to evaluate the effect of field of view. Our objectives were to understand the capacity for video methods to estimate Brook Trout *Salvelinus fontinalis* abundance and to assess the effects of physical habitat features and field of view on video performance in this regard.

METHODS

We used video, backpack electrofishing, and dive count methods to estimate juvenile (age-0) and adult (age-1 and older) Brook Trout abundance within 41 stream pools in Shenandoah National Park, Virginia (Figure 1). The study area is located within the Blue Ridge physiographic province of eastern North America and ranges in elevation from 320 to 1,230 m. Dominant vegetation is characterized by a mix of deciduous and coniferous forest cover. Both streams are located within the Chesapeake Bay watershed.

We sampled pools within the Staunton River ($n = 21$) and Paine Run ($n = 20$; Figure 1). Both streams are wadeable within the sample areas (i.e., maximum upstream basin size = 1,069 ha; Table 1), and geological parent material was primarily granitic (Staunton River) and siliciclastic (Paine Run; Jastram et al. 2013). The Staunton River was influenced by a major storm and debris flow event in 1995, resulting in short-term reductions in Brook Trout abundance (Roghair and Dolloff 2005) and alterations in benthic macroinvertebrate assemblage structure (Snyder and Johnson 2006). Both watersheds support spatially heterogeneous patterns of groundwater influence on stream temperature (Snyder et al. 2015) associated with landform features regulating groundwater–surface water interactions (Johnson et al. 2017, 2020).

We collected fish abundance data between September 25 and October 10, 2018, during base flow conditions. We selected sample sites following a systematic random design developed to characterize basinwide conditions (Hankin and Reeves 1988; Dolloff et al. 1993) such that we sampled every 10th pool from a randomized initial pool selection. We sampled sites in an upstream direction and conducted dive counts first, video sampling second, and electrofishing third. The interval between sampling methods typically exceeded 15 min. Pool density is lower in Paine Run than in the Staunton River (Newman 1995), and sample sites were more spread out in Paine Run as a result (Figure 1). Although Rainbow Trout *Oncorhynchus mykiss* and Brown Trout *Salmo trutta* occur in the study area (Jastram et al. 2013), Brook Trout were the only salmonids observed in sample sites.

Dive count surveys were conducted by a single observer moving upstream in each sample pool (Dolloff et al. 1993; Dunham et al. 2009; Thurow et al. 2012). Juvenile and
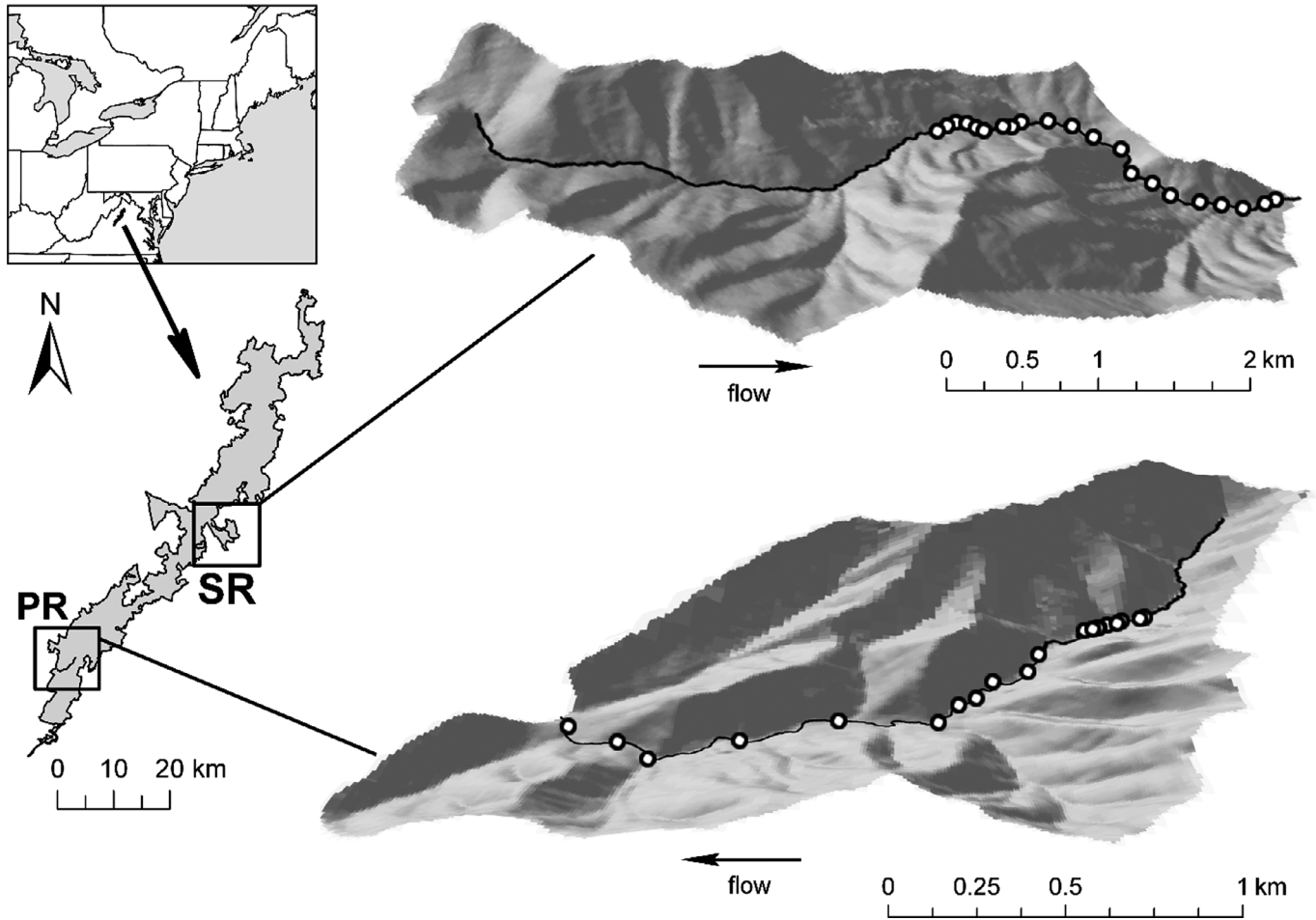
FIGURE 1. Study site locations in Shenandoah National Park, Virginia, USA ($n = 41$ pools). Study streams are abbreviated (SR = Staunton River; PR = Paine Run).

TABLE 1. Summary of environmental covariates among sample sites in Shenandoah National Park, Virginia ($n = 41$ pools). Pairwise correlations are given in the Supplemental Material (Table S1 available in the online version of this article).

Category	Environmental covariate	Units	Mean	SD	Range
Fish cover	Boulders	%	25.4	25.8	0.0–90.0
	Large woody debris	%	4.1	7.9	0.0–35.0
	Undercut banks	%	3.8	8.4	0.0–40.0
Geomorphology	Elevation	m	471.8	68.2	311–546
	Pool volume	m^3	21.7	18.8	1.7–85.3
	Riffle crest depth	cm	26.6	9.2	14.0–50.0
	Stream wetted width	m	6.1	2.0	3.2–10.7
	Upstream basin area	ha	599.9	281.7	83–1,069
Solar incidence	Canopy density	%	91.3	5.9	70.6–97.2

adult Brook Trout were counted separately based on attributes of body size, parr marks, and behavior. Blacknose Dace *Rhinichthys atratulus* commonly co-occur with Brook Trout in the study area (Jastram et al. 2013) but can be readily separated from trout based on body size, body shape, lateral pigmentation, and behavior (Jenkins and Burkhead 1994). The diver slowly moved upstream in the approximate center of each pool because conditions

enabled bank-to-bank observations underwater and prior research has demonstrated the utility of this method for sampling stream pools (Rodgers et al. 1992). Different divers sampled the Staunton River and Paine Run, and dive count relationships to electrofishing data for both observers were within the range observed from prior years of sampling (C. Krause, U.S. Forest Service [USFS], personal communication), thus minimizing potential observer-level effects. Both divers had prior experience conducting dive count surveys and were certified through USFS training. Although it can be difficult to identify species of juvenile trout during dive count surveys (Thurow 1994), this was not a concern in our study because only Brook Trout were present.

We collected video samples using "360°" waterproof cameras (360fly, New York) mounted on small tripods (Figure 2). The actual field of view encompassed 240°, but such cameras provide considerably larger views than others of similar size and cost (see Struthers et al. 2015). We also viewed video samples in "flat" mode to maximize field of view while reviewing videos for abundance estimates (see below). Cameras recorded 4K video resolution at rate of 50 Mbps with an aperture of F2.5 and a focal length of 0.88 mm. The cameras supported 64 GB of internal memory and approximately 1.5 h of recording time. Figure 3 provides a representative example of the video imagery we collected.

In each pool, we deployed two cameras simultaneously for 15 min. Cameras were positioned facing the thalweg on opposite sides of the sample area (Figure 2). We arbitrarily assigned camera 1 as the camera facing stream-right (i.e., located on stream-left) and camera 2 as the camera facing stream-left (i.e., located on stream-right) without respect to upstream or downstream location within pools. We did not incorporate an acclimation period (sensu Weyl et al. 2013) but instead used all video data to estimate fish abundance. Camera memory failure in one instance limited video samples to a single camera for four sites in Paine Run, yielding a total of 78 video samples for analysis. Of the 37 sites with video data from two cameras, 14 (38%) were small pools (i.e., mutually visible cameras) and 23 (62%) were large pools (i.e., cameras lacked mutual visibility).

We estimated fish abundance from each camera as the maximum count of individuals observed simultaneously in a video frame (MaxN). This method has been used previously in marine ecosystems (Ellis and DeMartini 1995; Cappo et al. 2007; Stoner et al. 2008; Gladstone et al. 2012; Campbell et al. 2018) and freshwater ecosystems (Ellender et al. 2012; Ebner and Morgan 2013; Weyl et al. 2013; Wilson et al. 2013; King et al. 2018). We also estimated juvenile and adult fish abundance for each pool with an integrated index between cameras (MaxNi) as

$$MaxNi = (MaxN_1 + MaxN_2) - N_{shared},$$

where $MaxN_1$ and $MaxN_2$ are the camera-level MaxN values, and N_{shared} is the count of individuals shared between camera-level MaxN values. We quantified N_{shared} based on the timing of fish movements, fish body size, and the location of common geomorphic features that were visible to both cameras. For example, we used boulder locations to infer fish movements from one camera to the other when the cameras were not mutually visible. We compared MaxN and MaxNi values against comparison methods to investigate the role of field of view in video sampling (i.e., larger for MaxNi than MaxN). One observer recorded all MaxN and N_{shared} values over a total of approximately 30 h (i.e., 45 min/site) by sequential viewing of camera 1 and camera 2 videos for each pool followed by time-specific comparisons to assess movement. Video analysis was conducted using a high-speed computing processor (Intel Xeon Gold 6140) and video card (NVIDIA Quadro P5000 with 16 GB).

After video sampling, USFS personnel conducted three-pass depletion sampling with a single backpack unit (Model AS2; Aqua Shock Solutions, Sevierville, Tennessee) and three dipnetters. Voltage ranged from 400 to 450 V, and duty cycle was 75% with 120 pulses/s. Stream conductivity was low, ranging from 7.5 to 19.0 μS/cm in the study area during summer 2018 (N. P. Hitt, unpublished data). Juvenile and adult Brook Trout were collected and counted for each pass, retained in buckets, and returned to the pool after the third pass. No mortalities were observed. We used pass-level counts to estimate latent abundance for both age-classes by using Carle and Strub (1978) depletion methods in the R package FSA version 0.8.23. Block nets were not used, but all available microhabitats were sampled with electricity during each pass. We evaluated electrofishing data as one-pass counts as well as three-pass estimates for comparison with video methods because both electrofishing methods are commonly used in stream fish research (Reynolds and Kolz 2012).

We measured environmental covariates in each pool to characterize fish cover, geomorphology, and canopy density (Table 1) after video sampling and before electrofishing. We assessed fish cover by visually estimating the percentage of pool area as undercut banks, submerged boulders, and submerged large woody debris (minimum diameter > 10 cm; Lazorchak et al. 1998). Stream wetted width, pool width, and pool length were measured to the nearest 0.1 m, and maximum pool depth and riffle crest depth were measured to the nearest centimeter. We estimated maximum pool volume by multiplying pool width, depth, and length values. Percent canopy density was estimated using spherical densiometers in accordance with Lemmon (1956). We used ArcHydro Tools (ESRI ArcGIS
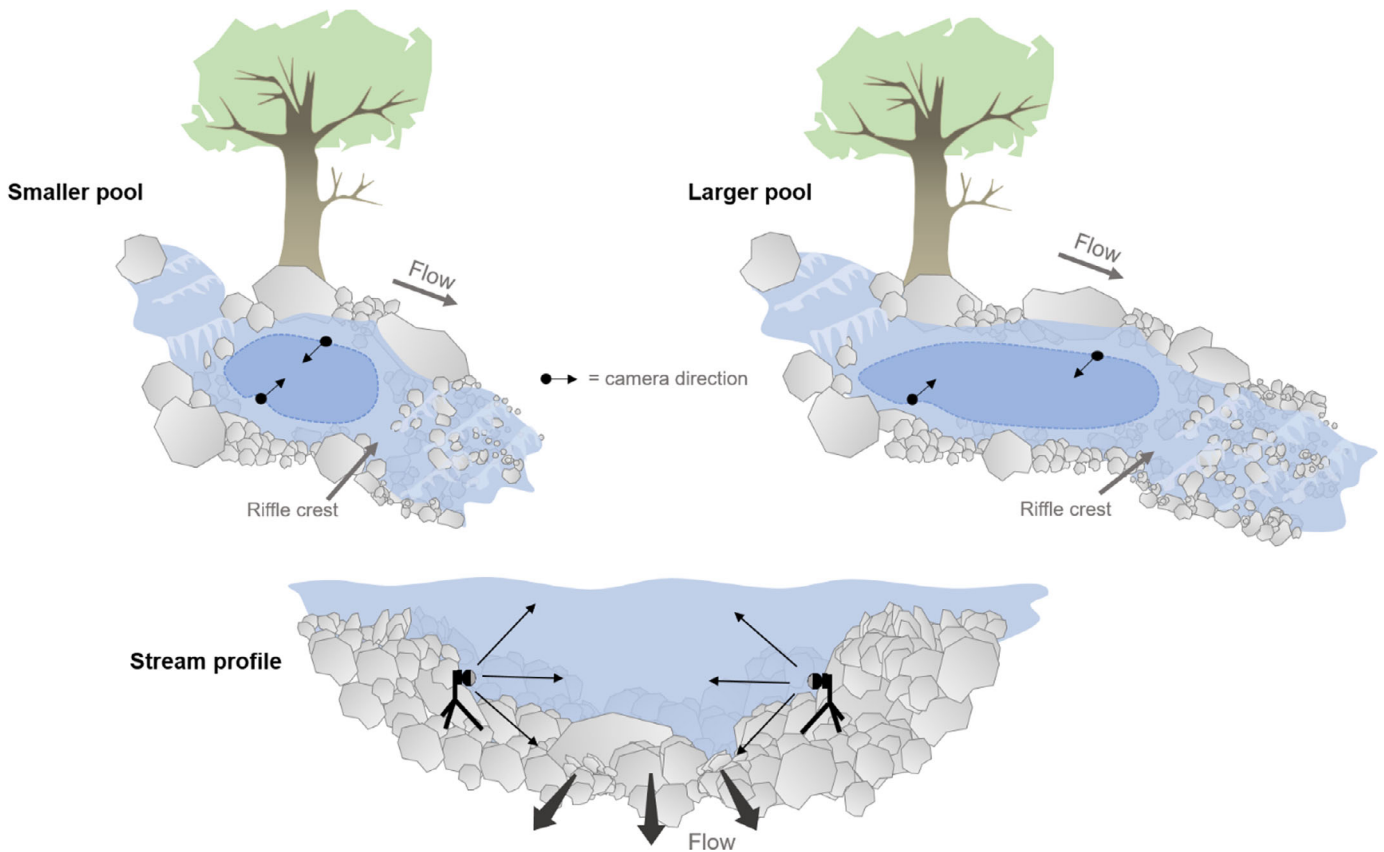
FIGURE 2. Camera placement schematic. Two cameras were placed along the lateral margin of each pool, facing the center of the stream. Cameras were mounted on small tripods to provide level imagery and to stabilize placement. [Color figure can viewed at afsjournals.org.]

FIGURE 3. Example of video imagery showing an adult Brook Trout in representative habitat conditions. Note the visibility of lateral fin margins for taxonomic identification.

Desktop version 10.6.1) to calculate elevation and upstream basin area for each site from a 10-m digital elevation map (USGS 2017).

We evaluated methodwise differences in trout abundance with two-sided t-tests assuming unequal group variance. We also evaluated 95% CIs from linear regression models and nonparametric locally weighted regression models (Cleveland 1979) to compare methods. We then calculated nonparametric correlations between linear model residuals and environmental covariates to evaluate the environmental basis of methodwise differences. All calculations were performed in R version 3.5.3 (R Core Team 2019).

RESULTS

Sampled pools encompassed elevations from 311 to 546 m and exhibited substantial variation in geomorphology and fish cover (Table 1). Pool volume ranged from 1.7 to 85.3 m³, and stream wetted width ranged from 3.2 to 10.7 m. Riffle crest depth averaged 26.6 cm and ranged from 14 to 50 cm. Sample sites included pools with and without boulders, large woody debris, and undercut banks (Table 1). Sites were highly forested, with an average of 91% canopy density. Several environmental covariates were correlated with basin area and elevation (see Table S1).

Estimates of juvenile Brook Trout abundance varied substantially among methods (Table 2; Figure 4). Electrofishing and dive counts estimated more juvenile fish

than video methods on average ($P < 0.03$; Table 2). In contrast, integrated video methods (*MaxNi*) estimated greater mean abundance of adult Brook Trout than did one-pass electrofishing counts ($P = 0.02$), and video results were not different from three-pass electrofishing in this regard ($P > 0.40$). Mean adult abundance was lower from camera-level estimates (*MaxN*) than from dive counts ($P < 0.10$; Table 2), but camera-level estimates of adult abundance were not significantly different from electrofishing results ($P \geq 0.10$; Table 2).

Regression models also showed that video methods underestimated juvenile Brook Trout abundance relative to other methods (Table 2). Linear model slopes for juvenile abundance ranged from 0.00 to 0.18 (Table 2), and 95% CIs for linear and locally weighted regression model predictions largely excluded the 1:1 relationships that define equal performance (Figure 5). Integrated video estimates for juvenile abundance (*MaxNi*) increased correspondence to comparison methods relative to camera-level estimates (*MaxN*), but methodwise linear model fit was low in all scenarios ($R^2 \leq 0.19$; Table 2). Results from individual cameras varied in their relationship to dive counts: the linear model slope for dive counts versus camera 2 was less than one-third that of dive counts versus camera 1 (Table 2).

In contrast, estimates of adult Brook Trout abundance were similar among methods (Table 2; Figure 4). Linear model slopes for adult abundance ranged from 0.13 to 1.44, and R^2 values ranged from 0.22 (*MaxN* for camera 2 versus one-pass electrofishing) to 0.75 (*MaxNi* versus dive counts; Table 2). Predicted 95% CIs for linear and locally weighted regression models of adult abundance approximated the 1:1 relationship for some video and electrofishing comparisons, but 95% CIs consistently excluded the 1:1 relationship between video methods and dive counts, as video counts were consistently lower (Figure 6). Conversely, 95% CIs exceeded the 1:1 relationship for adult abundance from video (*MaxNi*) versus one-pass electrofishing counts (Figure 6). Effects of influential points were apparent because 95% CIs for locally weighted regression predictions expanded across some high-abundance observations (Figure 6).

Integrated two-camera abundance estimates (*MaxNi*) showed closer correspondence to dive counts and electrofishing results than did single-camera estimates (*MaxN*; Table 2). For example, camera 1 and camera 2 slopes versus one-pass electrofishing counts were 1.09 and 0.42, respectively (Table 2). Of the 37 sites with video samples from two cameras, adult *MaxNi* values equaled the sum of camera-level *MaxN* values for 20 sites (54%), indicating no effect of fish movement in those sites (i.e., $N_{shared} = 0$). Conversely, adult *MaxNi* values were less than the sum of camera-level *MaxN* values for 17 sites (46%) by an average of 1.9 fish/site, indicating that integrated video

TABLE 2. Brook Trout abundance comparisons between video (*MaxN* = maximum count of individuals observed simultaneously in a video frame from camera 1 or camera 2; *MaxNi* = abundance index integrated between cameras) and electrofishing (EF; one pass or three passes) or dive count methods ($n = 41$ pools). Positive *t*-values indicate that abundance was greater in the video than in the comparison method and vice versa. Figures 5 and 6 plot the linear regression models.

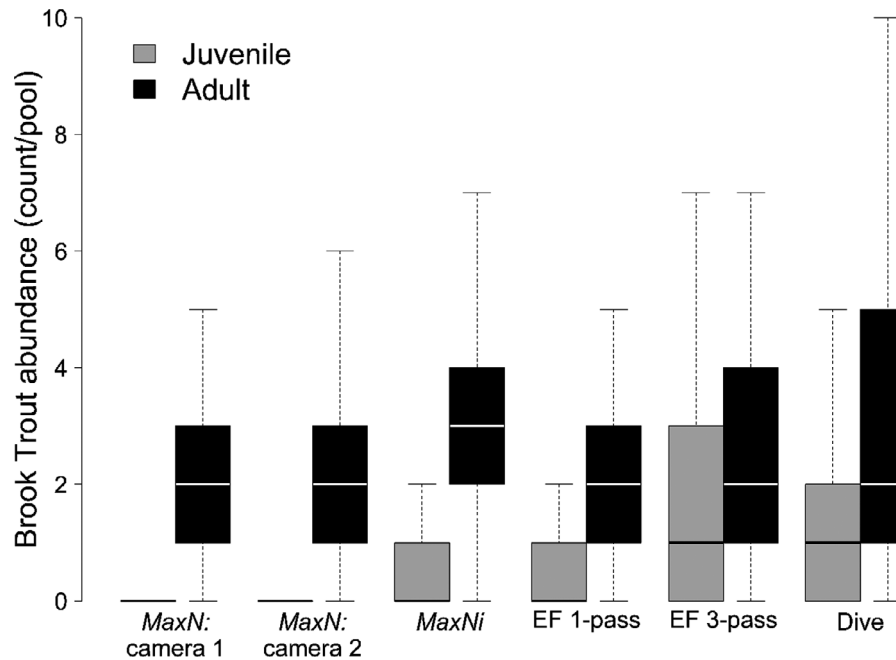| Age-class	Video method	Comparison method	*t*-tests		Linear regression models		
			t	*P*	Intercept	Slope	R^2
Juvenile	*MaxN*: camera 1	EF, one pass	−2.29	0.026	0.38	0.03	<0.01
	MaxN: camera 2		−3.00	0.004	0.22	0.01	<0.01
	MaxNi		−2.51	0.015	0.23	0.13	0.12
	MaxN: camera 1	EF, three passes	−2.77	0.008	0.38	0.02	0.01
	MaxN: camera 2		−3.14	0.003	0.24	0.00	<0.01
	MaxNi		−2.87	0.006	0.26	0.06	0.10
	MaxN: camera 1	Dive count	−3.65	0.001	0.12	0.18	0.13
	MaxN: camera 2		−4.45	<0.001	0.14	0.05	0.03
	MaxNi		−3.94	<0.001	0.12	0.16	0.19
Adult	*MaxN*: camera 1	EF, one pass	1.07	0.289	0.45	1.09	0.38
	MaxN: camera 2		0.20	0.844	1.22	0.42	0.26
	MaxNi		2.49	0.016	0.86	1.44	0.50
	MaxN: camera 1	EF, three passes	−0.52	0.604	0.19	0.80	0.61
	MaxN: camera 2		−1.67	0.100	1.22	0.27	0.31
	MaxNi		0.83	0.410	0.77	0.97	0.66
	MaxN: camera 1	Dive count	−1.73	0.088	0.49	0.47	0.69
	MaxN: camera 2		−2.52	0.015	1.48	0.13	0.22
	MaxNi		−0.72	0.472	1.14	0.57	0.75

FIGURE 4. Box plots for observed abundance of juvenile (age-0) and adult (age-1 and older) Brook Trout from video (*MaxN* = maximum count of individuals observed simultaneously in a video frame from camera 1 or camera 2; *MaxNi* = abundance index integrated between cameras), backpack electrofishing (EF; one pass or three passes), and dive count methods within stream pools.

methods accounted for movement of individuals between camera locations in these cases. Adult N_{shared} values ranged from 0 to 5 (mean = 0.9), and juvenile N_{shared} values ranged from 0 to 7 (mean = 0.2).

Environmental attributes of pool geomorphology, fish cover, and solar incidence were correlated with method-wise differences in adult Brook Trout abundance (Table 3). Linear model residuals for video methods versus one-pass electrofishing counts were positively correlated to boulder cover, riffle crest depth, stream wetted width, and upstream basin area ($P < 0.10$; Table 3). In contrast, residuals from the *MaxNi* video versus one-pass electrofishing model were negatively associated with the percentage of undercut banks in sample pools ($P < 0.05$). Residuals from video versus three-pass electrofishing models also were positively associated with boulder percent, riffle crest depth, and stream wetted width ($P < 0.10$), but residuals were negatively associated with canopy density ($P < 0.10$; Table 3). In contrast, video versus dive count model residuals were unrelated to environmental covariates ($P > 0.10$; Table 3).

The relationship between stream wetted width and linear model residuals varied between cameras (Table 3). For both one-pass and three-pass models, the camera facing stream-right (camera 1) showed a positive association with linear model residuals ($P < 0.10$), whereas the camera facing stream-left (camera 2) did not ($P > 0.10$; Table 3). Likewise, regression residuals showed a negative association with canopy density for one camera but not the other

(Table 3). Integrated video (*MaxNi*) model residuals showed stronger associations with boulder percent, riffle crest depth, and upstream basin area than single-camera abundance estimates (*MaxN*; Table 3). Environmental conditions explained absolute differences in adult Brook Trout abundance between integrated videos (*MaxNi*) and three-pass electrofishing (Table 3) because linear model residuals represented variation from a nearly 1:1 relationship (i.e., slope = 0.97; Table 2).

DISCUSSION

Our results demonstrated that underwater video samples can provide robust estimates of adult trout abundance in stream pools but may not effectively estimate juvenile trout abundance. We also showed an improvement in video performance with integrated two-camera estimates relative to single cameras, indicating the importance of an expanded field of view for fish abundance estimation in pools. Here, we discuss the ecological mechanisms underlying our results, recommendations and limitations for video sampling in stream pools, and potential future applications of video techniques in stream fish ecology.

Video techniques underestimated juvenile Brook Trout abundance relative to other methods, and we attribute this to predator avoidance behaviors by juvenile fish, limiting their use of camera-visible locations. Juvenile fish often move from deeper pool habitats to shallower riffle habitats with the introduction of predatory fish (Schlosser 1987).
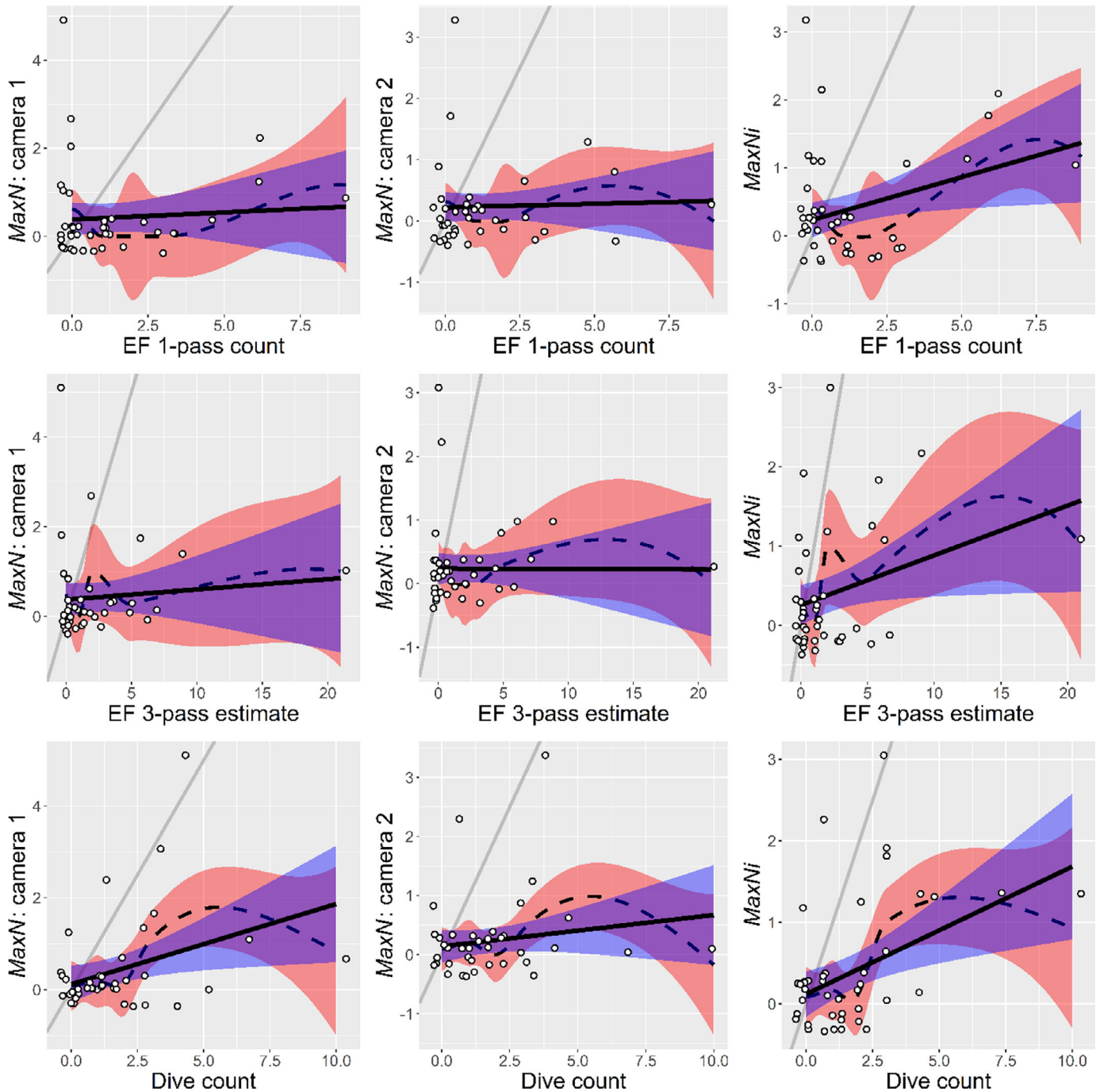
FIGURE 5. Comparison of juvenile (age-0) Brook Trout abundance estimates between video ($MaxN$ = maximum count of individuals observed simultaneously in a video frame from camera 1 or camera 2; $MaxNi$ = abundance index integrated between cameras) and backpack electrofishing (EF; one pass or three passes) or dive count methods within stream pools ($n = 41$). Gray lines show 1:1 relationships, black solid lines show linear model fits, and black dashed lines show locally weighted regression fits. Predicted 95% CIs are shown for linear models (blue) and locally weighted regression models (red). Note that points are jittered to reveal sample size (including some unobserved negative values). [Color figure can viewed at afsjournals.org.]

For instance, juvenile Bull Trout *Salvelinus confluentus* shifted their position into shallower habitats at the lateral margin of streams when adult Bull Trout immigrated into sites; juveniles then shifted back into deeper positions when adult trout emigrated (Pinto et al. 2013). Similarly, juvenile Brown Trout and Rainbow Trout tend to use shallow stream margins more often when predatory fish are present than when they are absent (Roussel and
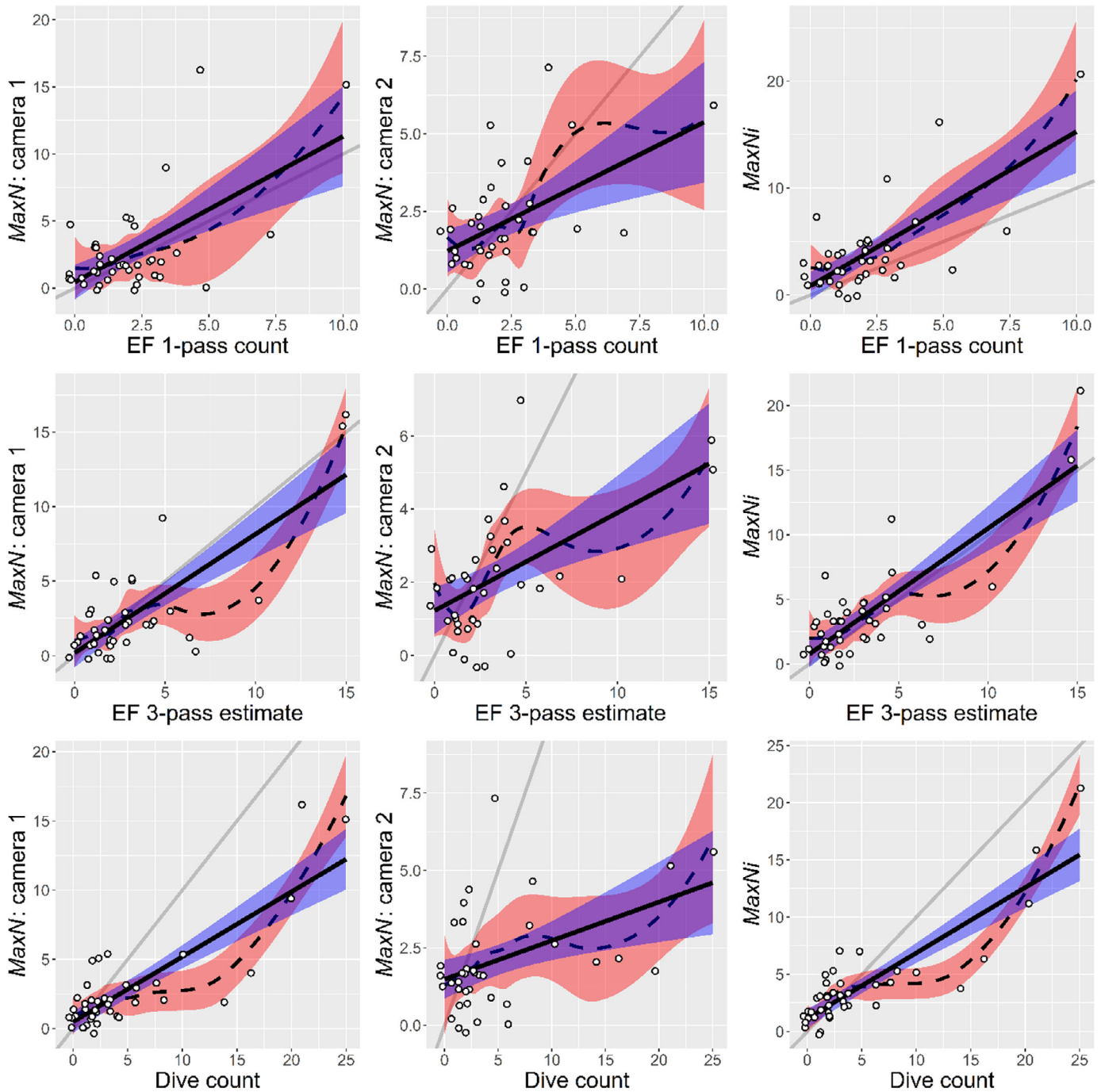
FIGURE 6. Comparison of adult (age-1 and older) Brook Trout abundance estimates between video (*MaxN* = maximum count of individuals observed simultaneously in a video frame from camera 1 or camera 2; *MaxNi* = abundance index integrated between cameras) and backpack electrofishing (EF; one pass or three passes) or dive count methods within stream pools (*n* = 41). Gray lines show 1:1 relationships, black solid lines show linear model fits, and black dashed lines show locally weighted regression fits. Predicted 95% CIs are shown for linear models (blue) and locally weighted regression models (red). Note that points are jittered to reveal sample size (including some unobserved negative values). [Color figure can viewed at afsjournals.org.]

Bardonnet 1999; Biro et al. 2003). Moreover, our video samples captured a period of high predation risk for juvenile trout because adult Brook Trout feed primarily during daylight hours (Allan 1981), their diet includes small fishes

(Jenkins and Burkhead 1994), and adult trout were observed in all of our sample pools. This observation may also explain why Frezza et al. (2003) and Ebner et al. (2015) found that video samples underestimated the

TABLE 3. Environmental associations with methodwise differences in adult Brook Trout abundance estimates (EF = electrofishing [one pass or three passes]; *MaxN* = maximum count of individuals observed simultaneously in a video frame from camera 1 or camera 2; *MaxNi* = abundance index integrated between cameras). Values are Spearman's rank correlation coefficients between environmental covariates (Table 1) and linear model residuals (see Table 2). Positive residuals indicate above-predicted abundance from video samples. Asterisks indicate the significance level of coefficients (*$P <$ 0.10; **$P < 0.05$). Variables with P-values greater than 0.10 are excluded.

		Video method		
Comparison method	Environmental covariate	*MaxN*: camera 1	*MaxN*: camera 2	*MaxNi*
EF, one pass	Boulders	0.17	0.10	0.37**
	Undercut banks	−0.24	−0.21	−0.32**
	Riffle crest depth	0.31*	0.18	0.28*
	Stream wetted width	0.28*	0.04	0.25
	Upstream basin area	0.18	0.12	0.34**
EF, three passes	Boulders	0.06	0.08	0.32**
	Riffle crest depth	0.23	0.25	0.29*
	Stream wetted width	0.31*	−0.05	0.16
	Canopy density	−0.29*	−0.20	−0.11

abundance of small-bodied fish in streams. However, our results in this regard may be limited to freshwater ecosystems given the lack of this effect reported from marine ecosystems (Coghlan et al. 2017) as well as the inherent difficulty in observing small fish via visual sampling methods (Thurow et al. 2012). Although our sampling design directed cameras toward the thalweg, additional cameras capturing stream margins may be better suited to detect juvenile trout for these reasons.

We found that integrated video data from two cameras (*MaxNi*) outperformed the data from single cameras (*MaxN*), and this may be due to competitive displacements from energetically profitable microhabitat locations. Pool locations that maximize access to incoming drift (i.e., food source) and minimize energetic requirements to hold a position in the water column are energetically profitable for fish (Fausch 1984). Competitive displacements from such energetically profitable microhabitats are common in salmonid fishes (Hitt et al. 2017; Cullen and Grossman 2019); therefore, competing fish may occupy a larger portion of the pool than would be visible to a single camera. Furthermore, because *MaxN* values are based on the simultaneous observation of aggregations of fish, competitive displacements may lead to underestimates of abundance if fish are displaced from energetically profitable locations, whereas the use of integrated multi-camera data may account for these effects. Campbell et al. (2018) demonstrated a similar result in marine ecosystems and recommended the use of 360° video systems for this purpose. Moreover, we demonstrated a method to avoid double-counting fish among cameras by accounting for shared individuals (N_{shared}) based on timing of movements, fish size, and the locations of natural landmarks that were visible to both cameras (e.g., boulders), thus addressing a

common pitfall in dive count methods (Thurow et al. 2012).

Our results further indicated that two cameras can provide sufficient coverage for the range of pool volumes we sampled (Table 1), in contrast to the four-camera method of Campbell et al. (2018) in marine ecosystems. Although marine environments may require averaging *MaxN* values over time to account for fish emigration and immigration (e.g., "MeanCount" sensu Schobernd et al. 2014), our results suggest that this is less of a concern for stream pools given their relatively small volume and the observed concordance between video and comparison methods for adult trout (Table 2). Although we cannot reject the possibility that fish moved into and out of sampled pools (i.e., block nets were not used), this is an unlikely explanation for our results because the time period between sampling methods in each pool typically exceeded the 5-min acclimation period applied elsewhere to estimate baseline conditions with video sampling (Weyl et al. 2013). Moreover, we demonstrated that methodwise differences in adult abundance were unrelated to pool volume (Table 3), indicating the utility of video methods across the observed range of pool sizes (Table 1).

We found that geomorphic attributes of pools can explain differences in method performance. Videos estimated more adult Brook Trout than electrofishing in several sites (Figure 6), and the magnitude of these differences (i.e., linear model residuals) increased with boulder composition and riffle crest depth (Table 3). This suggests that electrofishing capture efficiency decreases under these conditions due to fish escapement. Such imperfect detection is well known in abundance modeling (Kellner and Swihart 2014), and our results indicate that riffle crest depth and boulder composition could provide

useful covariates for modeling the fish detection process in a hierarchical framework (e.g., *N*-mixture models). Because backpack electrofishing typically is conducted at the reach scale (i.e., 100–1,000 m) rather than the pool scale (i.e., 1–10 m; Reynolds and Kolz 2012), upstream fish escapement (Peterson et al. 2005) may not hinder abundance estimates if fish are chased to a confining feature in the sample area where they are captured. However, riffle crest depth measures the depth of flow from the sample pool into the next downstream feature, suggesting downstream rather than upstream escapement in this case. This effect could bias electrofishing toward the underestimation of trout abundance if such geomorphic features were prevalent within the sampling reach.

In contrast to electrofishing, environmental conditions did not explain differences between dive counts and video methods. Water clarity and physical obstructions are well-known limitations for dive counts in assessing fish abundance (Northcote and Wilkie 1963; Young and Hayes 2001; Hayes et al. 2015); therefore, such environmental features may limit video methods in a similar fashion. Additionally, although we did not quantify water turbidity in sample sites, we would expect its effects to be equivalent between dive count and video methods because sampling was conducted without intervening rainfall events. However, we cannot reject the possibility that physical habitat disturbance from dive counts displaced some fish from the sample area, rendering them unavailable for subsequent video or electrofishing samples.

Our results indicate the utility of video techniques for a spatially intensive perspective on fish abundance within stream networks. Spatially intensive sampling may be particularly important in stream ecosystems that exhibit sharp gradients or discontinuities in local habitat characteristics influencing population structure and viability (Fausch et al. 2002). For instance, patchy groundwater–surface water interactions may affect stream thermal habitat (Snyder et al. 2015) based on spatially complex landform features regulating groundwater depth and flow paths (Johnson et al. 2017, 2020). Moreover, drought conditions can create fragmented stream networks that require intensive spatial sampling to understand fish population responses (Kovach et al. 2019). Spatially intensive sampling approaches have been used to assess fish abundance and fish habitat at the basin scale (Hankin and Reeves 1988; Dolloff et al. 1993), and our results further indicate the utility for video techniques at the stream network scale.

Our results also indicated some important limitations of video sampling. We found that video data were not useful for estimating juvenile trout abundance, likely due to predator avoidance behaviors, and we expect similar limitations for other small-bodied fishes in the presence of predatory trout. We also demonstrated the importance of

field of view for video data, and by extension we expect that video may not be useful for sampling riffle habitats with a restricted field of view due to shallow water and turbulence. In addition, video methods will be most effective for species with obvious coloration and body shape patterns, and we expect that video would be less useful for cryptic or nocturnal species, as reported by Ebner et al. (2015) and others. For example, American Eel *Anguilla rostrata* are present in the study streams (Hitt et al. 2012) but were not observed in any of our video samples. Similarly, we do not expect that video methods could reliably distinguish between closely related species that require detailed examinations or dissection for positive species identification (e.g., shiners *Notropis* spp.), as shown by others (Holmes et al. 2013; Branigan et al. 2018). Video methods also are subject to digital data loss, which was experienced here and was reported by Ebner et al. (2015). Moreover, video methods require substantial analysis time and computing capacity (see Methods), whereas dive and electrofishing methods yield immediate inferences on fish abundance.

Digital imagery shows great utility for fish species identification from artificial intelligence and machine learning algorithms (Boussarie et al. 2016; Salman et al. 2016, 2019; Qin et al. 2016; dos Santos and Gonçalves 2019; Willi et al. 2019), and our results further indicate its potential for estimating stream fish abundance and modeling population dynamics. For example, a recent study of estuarine fish populations found that computer-generated *MaxN* values were 7% more accurate than those provided by human observers (E. Ditria, Australian Rivers Institute, Southport, Queensland, personal communication), and machine learning models for species identification from imagery have recently achieved lower error rates than human observers (Wäldchen and Mäder 2018). Moreover, video techniques can enable citizen science and crowdsourcing methods to collect and analyze large ecological data sets (Marvin et al. 2016), such as those necessary to detect trends in Brook Trout abundance (Pregler et al. 2019). We anticipate that the integration of video methods with citizen science and machine learning models will facilitate powerful new directions in stream fish research, management, and conservation.

Ecosystems Mission Area, Chesapeake Bay studies, and Natural Resource Preservation Program. Any use of trade, firm, or product names is for descriptive purposes only and does not imply endorsement by the U.S. Government. There is no conflict of interest declared in this article.

REFERENCES

Allan, J. D. 1981. Determinants of diet of Brook Trout (*Salvelinus fontinalis*) in a mountain stream. Canadian Journal of Fisheries and Aquatic Sciences 38:184–192.

Becker, A. P., D. Cowley, and A. K. Whitfield. 2010. Use of remote underwater video to record littoral habitat use by fish within a temporarily closed South African estuary. Journal of Experimental Marine Biology and Ecology 391:161–168.

Biro, P. A., J. R. Post, and E. A. Parkinson. 2003. Population consequences of a predator-induced habitat shift by trout in whole-lake experiments. Ecology 84:691–700.

Boussarie, G., N. Teichert, R. Lagarde, and D. Ponton. 2016. Bichi-CAM, an underwater automated video tracking system for the study of migratory dynamics of benthic diadromous species in streams. River Research and Applications 32:1392–1401.

Branigan, P. R., M. C. Quist, B. B. Shepard, and S. C. Ireland. 2018. Comparison of a prepositioned areal electrofishing device and fixed underwater videography for sampling riverine fishes. Western North American Naturalist 78:65–75.

Brawn, V. M. 1960. Underwater television observations of the swimming speed and behaviour of captive herring. Journal of the Fisheries Research Board of Canada 17:689–698.

Campbell, M. D., J. Salisbury, R. Caillouet, W. B. Driggers, and J. Kilfoil. 2018. Camera field-of-view and fish abundance estimation: a comparison of individual-based model output and empirical data. Journal of Experimental Marine Biology and Ecology 501:46–53.

Cappo, M., G. De'ath, and P. Speare. 2007. Inter-reef vertebrate communities of the Great Barrier Reef Marine Park determined by baited remote underwater video stations. Marine Ecology Progress Series 350:209–222.

Carle, F. L., and M. R. Strub. 1978. A new method for estimating population size from removal data. Biometrics 34:621–630.

Castro-Santos, T. 2005. Optimal swim speeds for traversing velocity barriers: an analysis of volitional high-speed swimming behavior of migratory fishes. Journal of Experimental Biology 208:421–432.

Chaudoin, A. L., O. G. Feuerbacher, S. A. Bonar, and P. J. Barrett. 2015. Underwater videography outperforms above-water videography and in-person surveys for monitoring the spawning of Devils Hole Pupfish. North American Journal of Fisheries Management 35:1252–1262.

Cleveland, W. S. 1979. Robust locally weighted regression and smoothing scatterplots. Journal of the American Statistical Association 74:829–836.

Coghlan, A. R., D. L. McLean, E. S. Harvey, and T. J. Langlois. 2017. Does fish behavior bias abundance and length information collected by baited underwater video? Journal of Marine Biology and Ecology 497:143–151.

Cullen, J. L., and G. D. Grossman. 2019. Aggressive interactions affect foraging and use of space in a drift foraging salmonid, *Salvelinus malma* (Salmoniformes: Salmonidae). Zoological Journal of the Linnean Society 187:774–781.

Dean, J. C., A. J. Temple, and J. W. Smith. 2019. Output performance of U.S.-built backpack electrofishers. North American Journal of Fisheries Management 39:1321–1328.

Dolloff, C. A., D. G. Hankin, and G. H. Reeves. 1993. Basinwide estimation of habitat and fish populations in streams. U.S. Forest Service General Technical Report SE-83.

dos Santos, A. A., and W. N. Gonçalves. 2019. Improving Pantanal fish species recognition through taxonomic ranks in convolutional neural networks. Ecological Informatics 53:100977.

Dunham, J. B., A. E. Rosenberger, R. F. Thurow, C. A. Dolloff, and P. J. Howell. 2009. Coldwater fish in wadeable streams. Pages 119–138 *in* S. A. Bonar, W. A. Hubert, and D. W. Willis, editors. Standard methods for sampling North American freshwater fishes. American Fisheries Society, Bethesda, Maryland.

Ebner, B. C., C. J. Fulton, S. Cousins, J. A. Donaldson, M. J. Kennard, J. O. Meyncke, and J. Schaffer. 2015. Filming and snorkelling as visual techniques to survey fauna in difficult to access tropical rainforest streams. Marine and Freshwater Research 66:120–126.

Ebner, B. C., and D. L. Morgan. 2013. Using remote underwater video to estimate freshwater fish species richness. Journal of Fish Biology 82:1592–1612.

Ellender, B. R., A. Becker, O. L. F. Weyl, and E. R. Swartz. 2012. Using video analysis as a non-destructive alternative to electrofishing for sampling imperilled headwater stream fishes. Aquatic Conservation: Marine and Freshwater Ecosystems 22:58–65.

Ellis, D. M., and E. E. DeMartini. 1995. Evaluation of a video camera technique for indexing abundances of juvenile Pink Snapper, *Pristipomoides filamentosus*, and other Hawaiian insular shelf fishes. U.S. National Marine Fisheries Service Fishery Bulletin 93:67–77.

Fausch, K. D. 1984. Profitable stream positions for salmonids: relating specific growth rate to net energy gain. Canadian Journal of Zoology 62:441–451.

Fausch, K. D., C. E. Torgersen, C. V. Baxter, and H. W. Li. 2002. Landscapes to riverscapes: bridging the gap between research and conservation of stream fishes. BioScience 52:483–498.

Feyrer, F., D. Portz, D. Odum, K. B. Newman, T. Sommer, D. Contreras, R. Baxter, S. B. Slater, D. Sereno, and E. V. Nieuwenhuyse. 2013. SmeltCam: underwater video codend for trawled nets with an application to the distribution of the imperiled Delta Smelt. PLoS (Public Library of Science) One [online serial] 8:e67829.

Frezza, T. L., L. M. Carl, and S. M. Reid. 2003. Evaluation of a portable underwater video camera to study fish communities in two Lake Ontario tributaries. Journal of Freshwater Ecology 18:269–276.

Gladstone, W., S. Lindfield, M. Coleman, and B. Kelaher. 2012. Optimisation of baited remote underwater video sampling designs for estuarine fish assemblages. Journal of Experimental Marine Biology and Ecology 429:28–35.

Hankin, D. G., and G. H. Reeves. 1988. Estimating total fish abundance and total habitat area in small streams based on visual estimation techniques. Canadian Journal of Fisheries and Aquatic Sciences 45:834–844.

Hatch, D. R., J. K. Fryer, M. Schwartzberg, D. R. Pederson, and A. Wand. 1998. A computerized editing system for video monitoring of fish passage. North American Journal of Fisheries Management 18:694–699.

Hawkins, P. R., K. G. Hortle, S. Phommanivong, and Y. Singsua. 2018. Underwater video monitoring of fish passage in the Mekong River at Sadam Channel, Khone Falls, Laos. River Research and Applications 2018:1–12.

Hayes, J. W., J. Hay, I. Maxwell, and A. Quarterman. 2015. Estimating trout abundance with a cataraft-mounted dual-frequency identification sonar: a comparison with drift diving. North American Journal of Fisheries Management 35:528–536.

Hitt, N. P., S. Eyler, and J. E. B. Wofford. 2012. Dam removal increases American Eel abundance in distant headwater streams. Transactions of the American Fisheries Society 141:1171–1179.

Hitt, N. P., E. Snook, and D. Massie. 2017. Brook Trout use of thermal refugia and foraging habitat influenced by Brown Trout. Canadian Journal of Fisheries and Aquatic Sciences 74:406–418.

Holmes, T. H., S. K. Wilson, M. J. Travers, T. J. Langlois, R. D. Evans, G. I. Moore, R. A. Douglas, G. Shedrawi, E. S. Harvey, and K. Hickey. 2013. A comparison of visual- and stereo-video based fish community assessment methods in tropical and temperate marine waters of western Australia. Limnology and Oceanography: Methods 11:337–350.

Jastram, J. D., C. D. Snyder, N. P. Hitt, and K. C. Rice. 2013. Synthesis and interpretation of surface-water quality and aquatic biota data collected in Shenandoah National Park, Virginia, 1979–2009. U.S. Geological Survey, Scientific Investigations Report 2013-5157, Reston, Virginia.

Jenkins, R. E., and N. M. Burkhead. 1994. Freshwater fishes of Virginia. American Fisheries Society, Bethesda, Maryland.

Johnson, Z. C., B. G. Johnson, M. A. Briggs, W. D. Devine, C. D. Snyder, N. P. Hitt, D. K. Hare, and T. V. Minkova. 2020. Paired air–water annual temperature patterns reveal hydrogeological controls on stream thermal regimes at watershed to continental scales. Journal of Hydrology 587:124929.

Johnson, Z. C., C. D. Snyder, and N. P. Hitt. 2017. Landform features and seasonal precipitation predict shallow groundwater influence on temperature in headwater streams. Water Resources Research 53:5788–5812.

Kellner, K. F., and R. K. Swihart. 2014. Accounting for imperfect detection in ecology: a quantitative review. PLoS (Public Library of Science) One [online serial] 9:e111436.

King, A. J., A. George, D. J. Buckle, P. A. Novak, and C. J. Fulton. 2018. Efficacy of remote underwater video cameras for monitoring tropical wetland fishes. Hydrobiologia 807:145–164.

Kovach, R., J. Dunham, R. Al-Chokhachy, C. Snyder, J. Young, A. Lynch, C. Konrad, K. Jaeger, N. P. Hitt, B. Letcher, A. Rea, A. Sepulveda, G. Pederson, P. Lambert, C. Torgersen, J. Stoker, and C. Muhlfeld. 2019. An integrated framework for ecological drought across riverscapes of North America. BioScience 69:418–431.

Lazorchak, J. M., D. J. Klemm, and D. V. Peck. 1998. Environmental Monitoring and Assessment Program–surface waters: field operations and methods for measuring the ecological condition of wadeable streams. U.S. Environmental Protection Agency, Washington, D.C.

Lemmon, P. E. 1956. A spherical densiometer for estimating forest overstory density. Forest Science 2:314–320.

Mallet, D., and D. Pelletier. 2014. Underwater video techniques for observing coastal marine biodiversity. Fisheries Research 154:44–62.

Marvin, D. C., L. P. Koh, A. J. Lynam, S. Wich, A. B. Davies, R. Krishnamurthy, E. Stokes, R. Starkey, and G. P. Asner. 2016. Integrating technologies for scalable ecology and conservation. Global Ecology and Conservation 7:262–275.

Morán-López, R., and O. U. Tolosa. 2017. Image techniques in turbid rivers: a ten-year assessment of cyprinid stocks composition and size. Fisheries Research 195:186–193.

Moser, M. L., P. J. Auster, and J. B. Bichy. 1998. Effects of mat morphology on large *Sargassum* associated fishes: observations from a remotely operated vehicle (ROV) and free-floating video camcorders. Environmental Biology of Fishes 51:391–398.

Mueller, R. P., R. S. Brown, J. Hop, and L. Moulton. 2006. Video and acoustic camera techniques for studying fish under ice: a review and comparison. Reviews in Fish Biology and Fisheries 16:213–226.

Myrberg, A. A., A. Banner, and J. D. Richard. 1969. Shark attraction using a video-acoustic system. Marine Biology 2:264–276.

Newman, K. R. 1995. Response of Brook Char (*Salvelinus fontinalis*) and Blacknose Dace (*Rhinichthys atratulus*) to acidic episodes in three headwater streams within the Shenandoah National Park, Virginia. Master's thesis. Virginia Polytechnic Institute and State University, Blacksburg.

Northcote, T. G., and D. W. Wilkie. 1963. Underwater census of stream fish populations. Transactions of the American Fisheries Society 92:146–151.

Peterson, J. T., N. P. Banish, and R. F. Thurow. 2005. Are block nets necessary? Movement of stream-dwelling salmonids in response to three common survey methods. North American Journal of Fisheries Management 25:732–743.

Pinto, M. C., J. R. Post, A. J. Paul, F. D. Johnston, C. J. Mushens, and J. D. Stelfox. 2013. Lateral and longitudinal displacement of stream-rearing juvenile Bull Trout in response to upstream migration of spawning adults. Transactions of the American Fisheries Society 142:1590–1601.

Pregler, K. C., R. D. Hanks, E. Childress, N. P. Hitt, D. J. Hocking, B. H. Letcher, T. Wagner, and Y. Kanno. 2019. State-space analysis of power to detect regional Brook Trout population trends over time. Canadian Journal of Fisheries and Aquatic Sciences 76:2145–2155.

Qin, H., X. Li, J. Liang, Y. Peng, and C. Zhang. 2016. DeepFish: accurate underwater live fish recognition with a deep architecture. Neurocomputing 187:49–58.

R Core Team. 2019. R: a language and environment for statistical computing. R Foundation for Statistical Computing, Vienna.

Reynolds, J. B., and A. L. Kolz. 2012. Electrofishing. Pages 305–361 *in* A. V. Zale, D. L. Parrish, and T. M. Sutton, editors. Fisheries techniques, 3rd edition. American Fisheries Society, Bethesda, Maryland.

Rodgers, J. D., M. F. Solazzi, S. L. Johnson, and M. A. Buckman. 1992. Comparison of three techniques to estimate juvenile Coho Salmon populations in small streams. North American Journal of Fisheries Management 12:79–86.

Roghair, C. N., and C. A. Dolloff. 2005. Brook Trout movement during and after recolonization of a naturally defaunated stream reach. North American Journal of Fisheries Management 25:777–784.

Roussel, J. M., and A. Bardonnet. 1999. Ontogeny of diel pattern of stream margin habitat use by emerging Brown Trout, *Salmo trutta*, in experimental channels: influence of food and predator presence. Environmental Biology of Fishes 56:253–262.

Rowland, W. J., K. J. Bolyard, J. J. Jenkins, and J. Fowler 1995. Video playback experiments on stickleback mate choice: female motivation and attentiveness to male colour cues. Animal Behavior 49:1559–1567.

Salman, A., A. Jalal, F. Shafait, A. Mian, M. Shortis, J. Seager, and E. Harvey. 2016. Fish species classification in unconstrained underwater environments based on deep learning. Limnology and Oceanography: Methods 14:570–585.

Salman, A., S. Maqbool, A. H. Khan, A. Jalal, and F. Shafait. 2019. Real-time fish detection in complex backgrounds using probabilistic background modelling. Ecological Informatics 51:44–51.

Schlosser, I. J. 1987. The role of predation in age- and size-related habitat use by stream fishes. Ecology 68:651–659.

Schobernd, Z. H., N. M. Bacheler, and P. B. Conn. 2014. Examining the utility of alternative video monitoring metrics for indexing reef fish abundance. Canadian Journal of Fisheries and Aquatic Sciences 71:464–471.

Snyder, C. D., N. P. Hitt, and J. A. Young. 2015. Accounting for the influence of groundwater on the thermal sensitivity of headwater streams to climate change. Ecological Applications 25:1397–1419.

Snyder, C. D., and Z. B. Johnson. 2006. Macroinvertebrate assemblage recovery following a catastrophic flood and debris flows in an Appalachian mountain stream. Journal of the North American Benthological Society 25:825–840.

Snyder, D. E. 2003. Invited overview: conclusions from a review of electrofishing and its harmful effects on fish. Reviews in Fish Biology and Fisheries 13:445–453.

Stewart, C. T., and M. M. F. Lutnesky. 2014. Retardation of reproduction in the Red Shiner due to electroshock. North American Journal of Fisheries Management 34:463–470.

Stoner, A. W., B. J. Laurel, and T. P. Hurst. 2008. Using a baited camera to assess relative abundance of juvenile Pacific Cod: field and laboratory tests. Journal of Experimental Marine Biology and Ecology 354:202–211.

Struthers, D. P., A. J. Danylchuk, A. D. M. Wilson, and S. J. Cooke. 2015. Action cameras: bringing aquatic and fisheries research into view. Fisheries 40:502–512.

Thurow, R. F. 1994. Underwater methods for study of salmonids in the Intermountain West. U.S. Forest Service General Technical Report INT-307.

Thurow, R. F., C. A. Dolloff, and J. E. Marsden 2012. Visual observation of fish and aquatic habitat. Pages 781–817 *in* A. V. Zale, D. L. Parrish, and T. M. Sutton, editors. Fisheries techniques, 3rd edition. American Fisheries Society, Bethesda, Maryland.

Trudel, M., and D. Boisclair. 1996. Estimation of fish activity costs using underwater video cameras. Journal of Fish Biology 48:40–53.

USGS (U.S. Geological Survey). 2017. 1/3rd arc-second digital elevation models (DEMs)–USGS National Map 3DEP downloadable data collection. USGS, Reston, Virginia.

Valentin, S., P. Sempeski, Y. Souchon, and P. Gaudin. 1994. Short-term habitat use by young Grayling, *Thymallus thymallus* L., under variable flow conditions in an experimental stream. Fisheries Management and Ecology 1:57–65.

Wäldchen, J., and P. Mäder. 2018. Machine learning for image based species identification. Methods in Ecology and Evolution 9:2216–2225.

Weyl, O. L. F., B. R. Ellender, D. J. Woodford, and M. S. Jordan. 2013. Fish distributions in the Rondegat River, Cape Floristic Region, South Africa, and the immediate impact of rotenone treatment in an invaded reach. African Journal of Aquatic Science 38:201–209.

White, S. L., B. C. Kline, N. P. Hitt, and T. Wagner. 2019. Individual behaviour and resource use of thermally stressed Brook Trout *Salvelinus fontinalis* portend the conservation potential of thermal refugia. Journal of Fish Biology 95:1061–1071.

Willi, M., R. T. Pitman, A. W. Cardoso, C. Locke, A. Swanson, A. Boyer, M. Veldthuis, and L. Fortson. 2019. Identifying animal species in camera trap images using deep learning and citizen science. Methods in Ecology and Evolution 10:80–91.

Willis, T. J., and R. C. Babcock. 2000. A baited underwater video system for the determination of relative density of carnivorous reef fish. Marine and Freshwater Research 51:755–763.

Wilson, K. L., M. S. Allen, R. N. M. Ahrens, and M. D. Netherland. 2013. Use of underwater video to assess freshwater fish populations in dense submerged aquatic vegetation. Marine and Freshwater Research 66:10–22.

Young, R. G., and J. W. Hayes. 2001. Assessing the accuracy of drift-dive estimates of Brown Trout (*Salmo trutta*) abundance in two New Zealand rivers: a mark–resighting study. New Zealand Journal of Marine and Freshwater Research 35:269–275.

SUPPORTING INFORMATION

Additional supplemental material may be found online in the Supporting Information section at the end of the article.